See page 1404

A DNA Microarray-based Analysis of the Host Response to a Nonviral Gene Carrier: A Strategy for Improving the Immune Response

Hiroto Hatakeyama[1,2], Erika Ito[1], Momoko Yamamoto[1], Hidetaka Akita[1,2], Yasuhiro Hayashi[1], Kazuaki Kajimoto[1], Noritada Kaji[3], Yoshinobu Baba[3] and Hideyoshi Harashima[1,2]

[1]Faculty of Pharmaceutical Sciences, Hokkaido University, Sapporo, Japan; [2]Core Research for Educational Science and Technology (CREST), Japan Science and Technology Agency, Kawaguchi, Japan; [3]Graduate School of Engineering, Nagoya University, Nagoya, Japan

The purpose of this study was to investigate the host response to systemically administered lipid nanoparticles (NPs) encapsulating plasmid DNA (pDNA) in the spleen using a DNA microarray. As a model for NPs, we used a multifunctional envelope-type nano device (MEND). Microarray analysis revealed that 1,581 of the differentially expressed genes could be identified by polyethylene glycol (PEG)-unmodified NP using a threefold change relative to the control. As the result of PEGylation, the NP treatment resulted in the reduction in the expression of most of the genes. However, the expression of type I interferon (IFN) was specifically increased by PEGylation. Based on the microarray and a pathway analysis, we hypothesize that PEGylation inhibited the endosomal escape of NP, and extended the interaction of toll-like receptor-9 (TLR9) with CpG-DNA accompanied by the production of type I IFN. This hypothesis was tested by introducing a pH-sensitive fusogenic peptide, GALA, which enhances the endosomal escape of PEGylated NP. As expected, type I IFN was reduced and interleukin-6 (IL-6) remained at the baseline. These findings indicate that a carrier design based on microarray analysis and the manipulation of intracellular trafficking constitutes a rational strategy for reducing the host immune response to NPs.

Received 6 December 2010; accepted 26 January 2011; published online 8 March 2011. doi:10.1038/mt.2011.24

INTRODUCTION

The success of clinical gene therapy greatly depends on the development not only of efficient but also safe gene delivery systems.[1] Because of the ease of large-scale production and lack of a specific immune response unlike viral vectors, various types of nonviral gene delivery systems such as lipoplexes, polyplexes, and micelles have been developed, in attempts to improve the efficiency of *in vivo* gene expression.[2–4] However, innate immune responses are induced by the systemic administration of a lipoplex.[5] Unmethylated CpG motifs of plasmid DNA in a lipoplex have been reported to stimulate the innate immune response by interacting with host toll-like receptor-9 (TLR9), expressed in endosomes, and to trigger the release of inflammatory cytokines, such as tumor necrosis factor-α (TNF-α), interleukin-6 (IL-6) and IL-12, and type I interferon (IFN).[6] It was reported that a lipoplex containing either methylated CpG or non-CpG plasmid DNA (pDNA) reduced cytokine production, but the reduction was not complete.[5,7,8] Furthermore, cytokine production was not completely abolished in TLR9$^{-/-}$ mice after an intravenous (i.v.) administration of a lipoplex or in primary cultured macrophages from TLR9$^{-/-}$ mice after lipoplex treatment.[7,9] DNA-dependent activator of IFN-regulatory factor (DAI) has been identified as a cytosolic DNA sensor.[10] DAI, also known as Z-DNA binding protein-1 (ZBP1), recognizes double-stranded DNA (dsDNA) in a CpG-independent manner, which causes an TLR9-independent innate immune response.[11] These findings suggest that the immune reaction to a lipoplex is more complicated than previously thought. This appears to be true for viral vectors[12] as well, and an understanding of host responses to the systemic administration of a lipoplex is necessary for the successful and efficacious development of *in vivo* gene delivery systems. However, examining the production of certain types of cytokines after i.v. administration is not sufficient to guarantee the safety of a gene delivery system.

To address and solve this issue, gene expression profiling represents a promising approach to understanding the underlying mechanism of host responses.[13–19] Kay and coworkers reported that a DNA microarray-based comparison of the host response to adenoviral (Ad) and adeno-associated viral vectors revealed that the host recognition of capsid and DNA of adeno-associated viral is different from that of Ad.[13] This approach has been also applied to nonviral vectors in the form of toxicogenomics studies.[16–19] In the case of a polypropylenimine dendrimer based DNA complex, a microarray analysis revealed that gene expression in culture cells was altered by the generation of the dendrimer, and was dependent on the cell lines.[16] However, the response of a host to a systemically administrated nonviral gene vector has not been examined using this approach.

We recently developed a novel lipid nanoparticle (NP), a multifunctional envelope-type nano device (MEND), in which pDNA is condensed with a polycation, followed by encapsulation with

Correspondence: *Hideyoshi Harashima, Kita 12, Nishi 6, Kita-ku, Sapporo, Hokkaido 060-0812, Japan. E-mail: harasima@pharm.hokudai.ac.jp*

a lipid envelope.[20] In this study, an analysis of splenic expression profiles in mice was conducted after the intravenous injection of MENDs as an NP model, using a whole-genome DNA microarray. Since the spleen is the largest secondary lymphoid organ and contains tissue macrophages that are associated with an immune response after an intravenous injection of a lipoplex.[21] It was hypothesized that modification with PEG would confer biocompatibility for nonviral vectors, resulting in an improved safety.[22] It would permit us to predict whether PEGylation would change the gene expression profile by NP administration for the better. However, since only a few studies of the effect of PEGylation on host response have appeared, detailed information on the influence of PEGylation is not available. Therefore, we attempted to elucidate the effect of the PEGylation of NP (PEG-NP) on the host response.

RESULTS

Characterization of NPs

The average diameter and ζ-potential of the condensed pDNA/polyethyleneimine (PEI) complex particles were ~80 nm and −50 mV, respectively. The average diameters and ζ-potentials of the prepared NPs are summarized in **Table 1**. The PEG-unmodified NP was around 200 nm in diameter, and was highly positively charged due to the presence of a cationic lipid. PEG modification (PEG-NP) reduced the diameter of the NP and the positive charge was decreased, compared to an unmodified NP, as the result of the formation of a stable lamellar structure with a larger curvature and masking of the surface of the lipid envelope by the aqueous layer of the PEG moiety.[23] Modification of PEG-NP with chol-GALA (GALA-NP) slightly reduced the ζ-potential of the NP since GALA contains negatively charged glutamic acid residues, but it had no influence on the diameter.

Microarray data analysis

To understand what occurs in a host following the systemic administration of an NP and a PEG-NP, splenic gene expression profiles in mice were generated using whole-genome oligonucleotide microarrays. The spleen is the largest secondary lymphoid organ and is associated with the immune response.[21] Mice were injected *via* the tail vein with HEPES-buffered glucose (HBG), NP, or PEG-NP. After 2 hour, the spleen was collected and RNA prepared from the tissues, microarrays were then hybridized, as described in the Materials and Methods section. Using a threefold change relative to the HBG treatment as a criterion for differential expression, 1,581 genes were extracted from the administration of NP. A clustergram of these 1,581 genes is shown in **Figure 1**. The downregulated 402 genes resulting from the NP treatment, compared to HBG were classified in cluster 1, and the other 1,179 genes, which were upregulated by the NP treatment, were classified into clusters 2–5. In clusters 1, 3, and 5 (55.8%), the variation in gene expression as the result of the PEG-NP treatment were reduced compared to the corresponding value for NP, suggesting that PEGylation reduces the biological stimulation of NP after systemic administration. On the other hand, the gene expression in cluster 2 showed subtle alterations between NP and PEG-NP (42.7%). PEG-NP unexpectedly caused an increase in gene expression compared to NP, as shown in cluster 4 (1.5%).

Gene Ontology (GO) analysis is used to identify the molecular pathways and describe the biological processes of the transcript profiling data. Based on the GO analysis, the GO terms of "biological process" that were significantly over-represented in each cluster are shown in **Table 2**. The GO terms of the downregulated genes are related to cell division such as "cytokinesis," "mitosis," "M phase of mitotic cell cycle," differentiation and metabolism. On the other hand, the majority of GO terms for the upregulated genes in clusters 2–5 are mainly associated with "immune response," "response to biotic stimulus," "defense response," and related processes, which are generally associated with the immune system. These observations indicate that the characteristics of the upregulated genes and downregulated genes resulting from the NPs treatment were completely different.

We further listed the top 25 genes in order of greatly altered expression level by the NP treatment compared with HBG in each cluster, as shown in **Table 3**. The ratios of the gene expression level of PEG-NP/NP in clusters 1, 3, and 5 were improved, and the ratios in cluster 2 were comparable. However, the ratios for PEG-NP/NP in cluster 4 were greatly enhanced. In cluster 3, inflammatory cytokines such as *Il6* and *Ifng* are ranked higher with significantly lower levels of expression in the PEG-NP treatment compared to

Table 1 Physical properties of the prepared nanoparticles

	NP	PEG-NP	GALA-NP
Diameter (nm)	200 ± 11	132 ± 6	131 ± 2
ζ-potential (mV)	58 ± 12	13 ± 2	6 ± 2

The data are expressed as the mean ± SD. (n = 3).

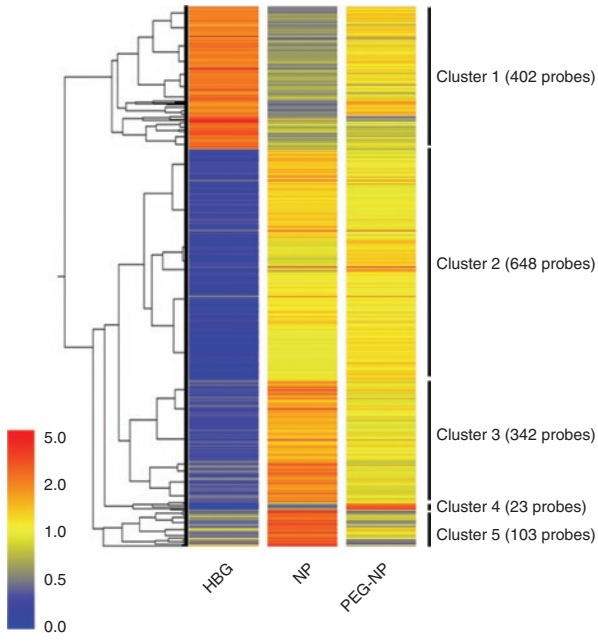

Figure 1 Clustergram of genes that are differentially regulated by administration of nanoparticles (NPs). 1,581 genes with an expression ratio of NP to HEPES-buffered glucose (HBG) >3 or <0.33 are represented. 402 genes were downregulated after NP administration, classified in cluster 1. The remaining 1,179 genes were upregulated, classified in clusters 2–5. Red, yellow, and blue represent relative gene expression among HBG, NP, and PEGylation of NP (PEG-NP).

Table 2 Statistically over-represented GO terms (biological Process) in each cluster

Category	Genes in category	Percent of genes in category	Genes in list in category	Percent of genes in list in category	*P* value
Cluster 1 (402 genes) P < 0.0001					
GO:35051: cardiac cell differentiation	8	0.0344	4	1.556	9.80×10^{-7}
GO:7571: age-dependent general metabolic decline	3	0.0129	3	1.167	1.33×10^{-6}
GO:1306: age-dependent response to oxidative stress	3	0.0129	3	1.167	1.33×10^{-6}
GO:910: cytokinesis	187	0.803	11	4.28	7.85×10^{-6}
GO:7067: mitosis	242	1.039	12	4.669	1.72×10^{-5}
GO:87: M phase of mitotic cell cycle	245	1.052	12	4.669	1.94×10^{-5}
GO:45494: photoreceptor maintenance	8	0.0344	3	1.167	7.14×10^{-5}
GO:51301: cell division	328	1.409	13	5.058	7.89×10^{-5}
GO:35050: embryonic heart tube development	22	0.0945	4	1.556	9.06×10^{-5}
Cluster 2 (648 genes) P < 10^{-12}					
GO:6955: immune response	835	3.586	102	27.35	6.38×10^{-61}
GO:9607: response to biotic stimulus	1,055	4.53	110	29.49	7.85×10^{-59}
GO:6952: defense response	1,010	4.337	108	28.95	8.61×10^{-59}
GO:9613: response to pest, pathogen, or parasite	450	1.932	48	12.87	1.49×10^{-25}
GO:43207: response to external biotic stimulus	505	2.169	48	12.87	2.35×10^{-23}
GO:9615: response to virus	44	0.189	19	5.094	4.77×10^{-23}
GO:50896: response to stimulus	3,266	14.02	122	32.71	1.90×10^{-20}
GO:50874: organismal physiological process	2,840	12.2	111	29.76	6.85×10^{-20}
GO:9605: response to external stimulus	778	3.341	51	13.67	1.11×10^{-17}
GO:8219: cell death	878	3.77	49	13.14	2.76×10^{-14}
GO:6915: apoptosis	817	3.508	47	12.6	3.23×10^{-14}
GO:16265: death	888	3.813	49	13.14	4.24×10^{-14}
GO:12501: programmed cell death	830	3.564	47	12.6	5.76×10^{-14}
GO:6954: inflammatory response	199	0.855	23	6.166	1.53×10^{-13}
GO:6950: response to stress	1,156	4.964	55	14.75	4.42×10^{-13}
Cluster 3 (342 genes) P < 10^{-8}					
GO:9607: response to biotic stimulus	1,055	4.53	45	20.36	1.36×10^{-17}
GO:6955: immune response	835	3.586	37	16.74	4.75×10^{-15}
GO:6952: defense response	1,010	4.337	40	18.1	1.33×10^{-14}
GO:43207: response to external biotic stimulus	505	2.169	26	11.76	2.81×10^{-12}
GO:9605: response to external stimulus	778	3.341	31	14.03	1.51×10^{-11}
GO:9613: response to pest, pathogen, or parasite	450	1.932	23	10.41	6.36×10^{-11}
GO:9611: response to wounding	365	1.567	20	9.05	3.56×10^{-10}
GO:6954: inflammatory response	199	0.855	14	6.335	7.44×10^{-9}
GO:45408: regulation of interleukin-6 biosynthesis	9	0.0386	5	2.262	8.99×10^{-9}
Cluster 4 (23 genes) P < 10^{-8}					
GO:9607: response to biotic stimulus	1,055	4.53	10	66.67	8.53×10^{-11}
GO:6952: defense response	1,010	4.337	10	66.67	5.55×10^{-11}
GO:43207: response to external biotic stimulus	505	2.169	5	33.33	1.18×10^{-5}
GO:9605: response to external stimulus	778	3.341	5	33.33	9.33×10^{-5}
GO:9613: response to pest, pathogen, or parasite	450	1.932	5	33.33	6.74×10^{-6}
GO:42830: defense response to pathogenic bacteria	10	0.0429	2	13.33	1.74×10^{-5}
GO:42829: defense response to pathogen	10	0.0429	2	13.33	1.74×10^{-5}
GO:9618: response to pathogenic bacteria	16	0.0687	2	13.33	4.62×10^{-5}

Table 2 Continued on next page

Table 2 Continued

Category	Genes in category	Percent of genes in category	Genes in list in category	Percent of genes in list in category	*P* value
GO:42828: response to pathogen	20	0.0859	2	13.33	7.31×10^{-5}
GO:50896: response to stimulus	3,266	14.02	11	73.33	3.21×10^{-7}
GO:9615: response to virus	44	0.189	3	20	2.82×10^{-6}
Cluster 5 (103 genes) $P < 10^{-8}$					
GO:16068: type I hypersensitivity	16	0.0687	6	9.375	2.66×10^{-12}
GO:6955: immune response	835	3.586	17	26.56	6.47×10^{-11}
GO:6952: defense response	1,010	4.337	18	28.12	1.38×10^{-10}
GO:9607: response to biotic stimulus	1,055	4.53	18	28.12	2.80×10^{-10}
GO:43207: response to external biotic stimulus	505	2.169	13	20.31	9.64×10^{-10}
GO:9613: response to pest, pathogen, or parasite	450	1.932	12	18.75	3.10×10^{-9}
GO:50874: organismal physiological process	2,840	12.2	26	40.62	8.70×10^{-9}

"Genes in list in category" represent the number of genes that were classified as the statistically over-represented Gene Ontology term.

NP. As shown in **Table 3**, *Ifna* subtypes and *Ifnb*, classified as type I IFN, are specifically located in cluster 4.

Quantification of mRNA level in spleen and cytokine level in serum

To verify that mRNA levels are elevated in the spleen, the mRNA expression of *Il6*, *Cd14*, located in cluster 3, and *Ifna* and *Ifnb*, located in cluster 4, the genes were further evaluated by quantitative reverse transcriptase-PCR (RT-PCR). As shown in **Figure 2**, the semiquantitative RT-PCR results were in good agreement with the expression information from the microarray analysis, confirming that these genes are actually upregulated after NP or PEG-NP administration. We next assessed the levels of IL-6 and IFN-α in serum at 2 and 6 hour after an i.v. injection of NP and PEG-NP. As shown in **Figure 3a**, NP induced the production of IL-6, and PEGylation markedly reduced the serum levels of IL-6. On the other hand, the serum level of IFN-α in the case of PEG-NP was equal or greater than that for NP. These observations were correlated with the amount of mRNA in the spleen, as evidenced by microarray analysis and quantitative PCR (**Figure 2**).

Pathway analysis and the effect of the acceleration of endosomal escape of PEGylated NP by GALA on type I IFN production

Based on the microarray analysis, PEGylation generally reduced the biological reaction to systemically administered NP. However, contrary to our expectations, PEGylation stimulated the production of type I IFN. To identify the mechanism underlying this, we performed a pathway analysis. According to the GO analysis and a subsequent quantitative determination of mRNA in the spleen, immune stimulation constituted a major biological reaction in the host after the systemic administration of NP. Since members of the TLR family are essential components in the CpG-mediated immune response, we focused on TLR pathway signaling using the Kyoto Encyclopedia of Genes and Genomes database. As shown in **Figure 4**, IL-6, IL-1β, and CD14, located in cluster 3 (red) and IFN-α and IFN-β, located in cluster 4 (blue) fall into TLR signaling pathway.

As described above, PEGylation confers biocompatibility and safety for NPs. On the other hand, it was reported that the modification of NP with PEG crucially inhibits the endosomal escape of NP,[24,25] resulting in a reduced activity of the cargo. We assumed that endosomal trapping triggered the excessive interaction of the pDNA encapsulated in PEG-NP with TLR9 following destabilization and digestion of the PEG-NP in endosomes/lysosomes, which resulted in an enhanced type I IFN production. We previously demonstrated that a pH-sensitive fusogenic peptide, GALA promoted the endosomal escape of PEGylated NP, which resulted in enhanced gene expression and silencing activity.[26–29] To test the assumption, we examined the effect of the GALA modification of PEG-NP (GALA-NP) on the immune response. The physical properties of the prepared GALA-NP were nearly the same as those for PEG-NP (**Table 1**). As shown in **Figure 5**, GALA modification successfully diminished serum IFN-α levels and IL-6 remained at a low level. The gene expression of *Ifna* in the spleen was also reduced by GALA modification.

DISCUSSION

In this study, we applied a microarray analysis to understand the host response to pDNA encapsulated in lipid NPs. For the microarray analysis, we used a MEND, in which pDNA is condensed with PEI, followed by encapsulation with a lipid envelope consisting of 1,2-dioleoyl-3-trimethylammonium-propane (DOTAP), dioleoylphosphatidyl ethanolamine (DOPE), and cholesterol. The systemic administration of the PEI/pDNA complex alone induced severe hepatotoxicity, but the innate immune response was negligible, unlike NPs (**Supplementary Figure S1**). These findings suggest that pDNA/PEI complex was successfully encapsulated by the lipid envelope of the MEND. These findings were also consistent with previous findings reported by Kawakami *et al.* in which a linear PEI polyplex showed negligible cytokine production and higher serum alanine transaminase levels after i.v. injection as compared with a N-[1-(2,3-dioleyloxy)propyl]-N,N,N-trimethylammonium chloride (DOTMA) based lipoplex.[30,31] From this viewpoint, the MENDs can be thought of as a model of an NP.

The microarray analysis showed that, after the systemic administration of NPs, the upregulated genes in the spleen were mainly

Table 3 Genes that are differentially expressed in response to nanoparticle treatment in each cluster

				Raw data			Ratio	
Probe ID	Description	UniGene	Genbank	HBG	NP	PEG-NP	NP/ HBG	PEG-NP/ NP
Cluster 1								
A_52_P122891	G protein-coupled receptor 154 (*Gpr154*)	Mm.130824	NM_175678	6,320	645	1,479	0.10	2.29
A_51_P480169	Endothelial differentiation, sphingolipid G-protein-coupled receptor, 8 (*Edg8*)	Mm.190619	NM_053190	732	104	170	0.14	1.63
A_51_P442894	RIKEN full-length clone:C130048D07	Mm.266843	AK048310	1,205	172	491	0.14	2.86
A_51_P164539	Armadillo repeat gene deleted in velo-cardio-facial syndrome (*Arvcf*)	Mm.293599	NM_033474	699	118	171	0.17	1.45
A_51_P370678	Growth factor independent 1B (*Gfi1b*)	Mm.373385	NM_008114	20,713	3,503	5,601	0.17	1.60
A_51_P472274	SRY-box containing gene 18 (*Sox18*)	Mm.264904	NM_009236	1,598	273	506	0.17	1.85
A_52_P495869	V-maf musculoaponeurotic fibrosarcoma oncogene family, protein B (avian) (*Mafb*)	Mm.330745	NM_010658	9,821	1,777	1,203	0.18	0.68
A_52_P28960	Growth differentiation factor 6 (*Gdf6*)	Mm.302555	NM_013526	930	179	263	0.19	1.47
A_51_P228792	cDNA sequence BC020025	Mm.273254	NM_146030	1,526	295	279	0.19	0.95
A_52_P563917	cDNA sequence BC019731	Mm.46582	NM_144914	1,048	204	895	0.19	4.39
A_52_P110052	Duffy blood group (*Dfy*)	Mm.6393	NM_010045	2,888	575	1,181	0.20	2.05
A_51_P217498	Solute carrier family 2 (facilitated glucose transporter), member 4 (*Slc2a4*)	Mm.10661	NM_009204	4,426	888	1,867	0.20	2.10
A_51_P340226	Sh3 domain YSC-like 1 (*Sh3yl1*)	Mm.218624	NM_013709	3,304	684	1,390	0.21	2.03
A_52_P449417	Vang, van gogh-like 1 (Drosophila)	Mm.331266	BC024687	3,020	634	1,262	0.21	1.99
A_51_P311611	Duffy blood group (*Dfy*)	Mm.6393	NM_010045	1,361	291	628	0.21	2.16
A_52_P565396	Histocompatibility 2, Q region locus 2 (*H2-Q2*)	Mm.33263	NM_010392	1,569	339	472	0.22	1.40
A_51_P389421	Fumarylacetoacetate hydrolase domain containing 1 (*Fahd1*)	Mm.347964	NM_023480	5,281	1,152	1,789	0.22	1.55
A_52_P219473	Cell division cycle 6 homolog (*S. cerevisiae*) (*Cdc6*)	Mm.20912	NM_011799	2,971	652	1,098	0.22	1.68
A_51_P354526	RIKEN cDNA 2010011I20 gene	Mm.30013	NM_025912	513	113	205	0.22	1.82
A_52_P276529	Ankyrin repeat domain 9 (*Ankrd9*)	Mm.250989	NM_175207	801	177	247	0.22	1.39
A_52_P276525	Ankyrin repeat domain 9 (*Ankrd9*)	Mm.250989	NM_175207	2,907	645	925	0.22	1.43
A_51_P514270	RIKEN full-length clone:2900072M03	Mm.104155	AK013768	1,497	334	701	0.22	2.10
A_51_P398525	Fructosamine 3 kinase (*Fn3k*)	Mm.266448	NM_022014	16,726	3,751	7,511	0.22	2.00
A_51_P170178	UDP-Gal:betaGal beta 1,3-galactosyltransferase polypeptide 7 (*B7galt7*)	Mm.192369	NM_146184	1,235	280	263	0.23	0.94
A_51_P501840	DnaJ (Hsp40) homolog, subfamily B, member 3 (*Dnajb3*)	Mm.3075	NM_008299	2,864	659	1,100	0.23	1.67
Cluster 2								
A_52_P676403	Chemokine (C-X-C motif) ligand 11 (*Cxcl11*)	Mm.131723	NM_019494	14	13,085	9,038	938.67	0.69
A_51_P123630	Immune-responsive gene 1 (*Irg1*)	Mm.4662	L38281	71	29,771	17,509	417.14	0.59
A_51_P123625	RIKEN full-length clone:9830109K16	Mm.4662	AK036446	84	33,973	20,103	404.06	0.59
A_51_P286737	Chemokine (C-C motif) ligand 2 (*Ccl2*)	Mm.290320	NM_011333	362	106,967	68,653	295.57	0.64
A_51_P436652	Chemokine (C-C motif) ligand 7 (Ccl7)	Mm.341574	NM_013654	15	4,271	1,943	290.54	0.45
A_51_P337308	Serum amyloid A 3 (*Saa3*)	Mm.14277	NM_011315	9	2,326	1,290	268.34	0.55
A_51_P184484	Matrix metalloproteinase 13 (*Mmp13*)	Mm.5022	NM_008607	56	10,257	6,863	182.38	0.67
A_52_P614259	Myxovirus (influenza virus) resistance 1 (*Mx1*)	Mm.33996	NM_010846	29	3,784	3,860	128.80	1.02
A_52_P446431	Myxovirus (influenza virus) resistance 1 (*Mx1*)	Mm.33996	NM_010846	103	12,169	12,008	118.49	0.99
A_52_P249514	Chemokine (C-C motif) ligand 12 (*Ccl12*)	Mm.867	NM_011331	21	2,451	2,452	114.59	1.00
A_52_P208763	Chemokine (C-C motif) ligand 7 (*Ccl7*)	Mm.341574	NM_013654	18	1,898	839	107.35	0.44

Table 3 Continued on next page

Table 3 Continued

Probe ID	Description	UniGene	Genbank	Raw data			Ratio	
				HBG	NP	PEG-NP	NP/HBG	PEG-NP/NP
A_52_P550858	RIKEN full-length clone:D630022O22	Mm.30756	AK085407	14	1,434	1,248	106.14	0.87
A_51_P385812	Interleukin 12b (Il12b)	Mm.239707	NM_008352	32	2,820	1,833	89.07	0.65
A_51_P279606	Suppressor of cytokine signaling 1 (*Socs1*)	Mm.130	NM_009896	2,821	245,879	140,246	87.16	0.57
A_51_P509573	Chemokine (C-C motif) ligand 4 (*Ccl4*)	Mm.244263	NM_013652	487	41,709	47,695	85.64	1.14
A_51_P514085	Myxovirus (influenza virus) resistance 2 (*Mx2*)	Mm.14157	NM_013606	735	61,688	53,591	83.94	0.87
A_52_P653054	Unknown	—	—	1,589	118,529	128,723	74.59	1.09
A_52_P663686	RIKEN full-length clone:5031412D17	Mm.271850	AK077243	231	15,706	17,600	67.99	1.12
A_51_P359570	Interferon-induced protein with tetratricopeptide repeats 3 (*Ifit3*)	Mm.271850	NM_010501	1,989	125,337	135,173	63.02	1.08
A_52_P452689	Activating transcription factor 3 (*Atf3*)	Mm.2706	NM_007498	289	17,030	11,720	58.89	0.69
A_51_P315785	Tumor necrosis factor alpha induced protein 6 (*Tnfaip6*)	Mm.3509	NM_009398	21	1,113	583	53.59	0.52
A_52_P947847	RIKEN full-length clone:A530076D18	Mm.254989	AK041062	5	267	157	52.03	0.59
A_52_P1016836	Tetratricopeptide repeat protein 6 (TPR repeat protein 6)	Mm.84118	XM_126988	3	166	254	49.52	1.53
A_52_P542388	Interferon-induced protein with tetratricopeptide repeats 2 (*Ifit2*)	Mm.2036	NM_008332	87	4,310	5,239	49.43	1.22
A_51_P327751	Interferon-induced protein with tetratricopeptide repeats 1 (*Ifit1*)	Mm.6718	NM_008331	1,184	58,059	57,029	49.04	0.98
Cluster 3								
A_51_P217218	Interleukin-6 (*Il6*)	Mm.1019	NM_031168	26	25,059	5,883	949.92	0.23
A_51_P363187	Chemokine (C-X-C motif) ligand 1 (*Cxcl1*)	Mm.21013	NM_008176	27	24,022	2,221	880.57	0.09
A_51_P220976	Interferon gamma (*Ifng*)	Mm.240327	NM_008337	167	87,420	10,721	524.73	0.12
A_52_P68893	Interferon gamma (*Ifng*)	Mm.240327	NM_008337	287	110,858	16,703	386.53	0.15
A_51_P217463	Chemokine (C-X-C motif) ligand 2 (*Cxcl2*)	Mm.4979	NM_009140	7	2,635	333	374.88	0.13
A_51_P455326	Selectin, endothelial cell (*Sele*)	Mm.5245	NM_011345	4	1,218	317	323.25	0.26
A_52_P177054	Interleukin 22 (*Il22*)	Mm.103585	NM_016971	3	957	37	304.91	0.04
A_51_P234944	A disintegrin-like and metalloprotease (reprolysin type) with thrombospondin type 1 motif, 4 (Adamts4)	Mm.23156	NM_172845	27	5,044	1,633	190.12	0.32
A_51_P171075	Colony stimulating factor 2 (granulocyte-macrophage) (*Csf2*)	Mm.4922	NM_009969	14	1,602	258	112.42	0.16
A_51_P427794	Actin binding LIM protein family, member 3 (*Ablim3*)	Mm.329478	NM_198649	12	1,058	157	85.05	0.15
A_51_P254855	Prostaglandin-endoperoxide synthase 2 (*Ptgs2*)	Mm.292547	NM_011198	4	295	62	76.52	0.21
A_52_P224760	Prostaglandin-endoperoxide synthase 2 (*Ptgs2*)	Mm.292547	NM_011198	4	259	57	69.23	0.22
A_52_P295432	Chemokine (C-X-C motif) ligand 5 (*Cxcl5*)	Mm.4660	NM_009141	138	8,986	1,470	65.26	0.16
A_51_P169908	RIKEN full-length clone:A130019G07	Mm.297393	AK037442	3	193	85	56.61	0.44
A_51_P138510	Granzyme C (*Gzmc)*	Mm.14465	NM_010371	12	654	74	56.31	0.11
A_51_P183571	Serine (or cysteine) proteinase inhibitor, clade E, member 1 (Serpine1)	Mm.250422	NM_008871	101	3,888	1,815	38.34	0.47
A_52_P329207	Extracellular proteinase inhibitor (*Expi*)	Mm.1650	NM_007969	41	1,430	164	35.03	0.11
A_51_P111164	Rho family GTPase 1 (*Rnd1*)	Mm.274010	NM_172612	1,671	57,998	17,710	34.71	0.31
A_51_P331752	Small chemokine (C-C motif) ligand 11 (*Ccl11*)	Mm.4686	NM_011330	28	934	176	33.81	0.19
A_51_P165182	RIKEN cDNA 4933430F08 gene	Mm.159219	NM_028967	711	23,794	10,839	33.45	0.46
A_51_P430766	Interleukin 10 (*Il10*)	Mm.874	NM_010548	22	624	156	28.62	0.25
A_51_P172853	CD14 antigen (Cd14)	Mm.3460	NM_009841	1,393	38,202	11,707	27.42	0.31

Table 3 Continued on next page

Table 3 Continued

Probe ID	Description	UniGene	Genbank	Raw data			Ratio	
				HBG	NP	PEG-NP	NP/HBG	PEG-NP/NP
A_51_P474459	Suppressor of cytokine signaling 3 (*Socs3*)	Mm.3468	NM_007707	6,010	158,332	74,355	26.34	0.47
A_52_P26161	Pentraxin related gene (*Ptx3*)	Mm.276776	NM_008987	3	85	26	25.18	0.31
A_52_P510387	RIKEN full-length clone:D230024E06	—	AK051959	3	78	32	23.57	0.41
Cluster 4								
A_51_P192930	Interferon alpha family, gene 6 (*Ifna6*)	Mm.377090	NM_008335	36	685	4,873	19.16	7.12
A_51_P355382	Interferon alpha family, gene 13 (*Ifna13*)	Mm.246592	NM_177347	83	1,195	7,901	14.41	6.61
A_51_P436401	Interferon alpha family, gene 1 (*Ifna1*)	Mm.57127	NM_010502	16	2,381	15,577	147.70	6.54
A_51_P465436	Interferon alpha family, gene B (*Ifnab*)	Mm.377093	NM_008336	12	1,926	12,087	154.95	6.28
A_51_P387681	Interferon alpha family, gene B (*Ifnab*)	Mm.377093	NM_008336	72	1,872	11,539	26.12	6.16
A_52_P211172	Interferon alpha family, gene 12 (*Ifna12*)	Mm.246618	NM_177361	14	4,494	27,667	330.93	6.16
A_52_P482280	Mouse alpha-interferon (MuIFN-alpha), 3′ cds & untranslated mRNA	Mm.14091	K01411	4	2,324	14,123	562.85	6.08
A_52_P931374	RIKEN full-length clone:C130037M17	Mm.1571	AK048149	3	14	78	4.16	5.74
A_51_P355829	Interferon alpha family, gene 4 (*Ifna4*)	Mm.377088	NM_010504	4	1,038	5,723	267.46	5.51
A_51_P363308	Interferon alpha family, gene 9 (*Ifna9*)	Mm.377092	NM_010507	138	845	4,601	6.14	5.45
A_52_P13337	Unknown	—	—	331	1,502	8,085	4.54	5.38
A_52_P602847	Glycosylation dependent cell adhesion molecule 1 (*Glycam1*)	Mm.219621	NM_008134	4	40	212	11.04	5.32
A_51_P144180	Interferon beta 1, fibroblast (*Ifnb1*)	Mm.1245	NM_010510	4	5,954	22,857	1356.57	3.84
A_51_P326826	Melanoma antigen (*Mela*)	Mm.270157	NM_008581	229	4,200	14,885	18.36	3.54
A_51_P243514	Hypothetical protein	Mm.31376	XM_138397	5	23	68	5.05	2.99
A_52_P22324	Phospholamban (*Pln*)	Mm.34145	NM_023129	13	44	131	3.49	2.97
A_51_P427953	Olfactory receptor 869 (*Olfr869*)	Mm.334988	NM_146557	3	28	64	7.97	2.30
A_52_P63739	Antimicrobial peptide RYA3 (*Rya3*)	Mm.55392	NM_194357	3	27	60	8.17	2.25
A_51_P338963	Unknown	—	—	7	42	93	5.84	2.19
A_52_P177699	Transcription factor 2 (*Tcf2*)	Mm.7226	NM_009330	11	63	107	5.66	1.71
A_52_P461105	G protein-coupled receptor 31, D17Leh66c region (*Gpr31c*)	Mm.335670	NM_001013832	8	36	60	4.32	1.66
A_51_P215143	RIKEN full-length clone:D430006K04	Mm.45514	AK084893	14	43	60	3.21	1.39
A_52_P367034	Tripartite motif protein 34 (*Trim34*)	Mm.263478	NM_030684	361	1,157	1,564	3.20	1.35
Cluster 5								
A_51_P461703	Major urinary protein 1 (*Mup1*)	Mm.237772	NM_031188	4	922	17	228.54	0.02
A_51_P317176	Colony stimulating factor 3 (granulocyte) (*Csf3*)	Mm.1238	NM_009971	4	760	19	184.20	0.03
A_51_P232628	Interleukin 22 (*Il22*)	Mm.103585	NM_016971	4	498	18	134.29	0.04
A_51_P160713	Albumin 1 (*Alb1*)	Mm.16773	NM_009654	4	290	6	72.18	0.02
A_51_P211334	UDP-Gal:betaGal beta 1,3-galactosyltransferase, polypeptide 6 (*B3galt6*)	Mm.347395	NM_080445	358	12,044	707	33.68	0.06
A_51_P229217	RIKEN full-length clone:D130011C11	—	AK083791	3	109	3	32.24	0.03
A_52_P554143	Unknown	—	—	3	96	7	29.60	0.07
A_52_P1100477	RIKEN full-length clone:C130095H06	Mm.374840	AK082018	6	161	8	26.76	0.05
A_52_P45399	Unknown	—	—	4	105	3	26.71	0.03
A_51_P258806	RIKEN full-length clone:2310020F24	Mm.121859	AK009417	33	784	58	23.62	0.07
A_52_P170685	Unknown	—	—	4	97	4	23.16	0.04
A_52_P232813	Gene model 1960, (NCBI) (Gm1960)	Mm.244289	NM_203320	6	121	11	21.53	0.09
A_52_P348256	Major urinary protein 1	Mm.237772	BC037152	4	84	9	20.99	0.11

Table 3 Continued on next page

Table 3 Genes that are differentially expressed in response to nanoparticle treatment in each cluster

Probe ID	Description	UniGene	Genbank	Raw data			Ratio	
				HBG	NP	PEG-NP	NP/HBG	PEG-NP/NP
A_51_P266883	Major urinary protein 4 (*Mup4*)	Mm.34335	NM_008648	27	554	43	20.50	0.08
A_52_P1043817	RIKEN full-length, clone:A630095O09	Mm.360357	AK042484	3	64	3	20.23	0.04
A_51_P180314	RIKEN full-length clone:2610016E04	Mm.237772	AK011413	4	79	7	19.76	0.09
A_52_P139439	Unknown	—	—	4	78	9	18.90	0.12
A_52_P342860	Esterase 1 (*Es1*)	Mm.88078	NM_007954	3	63	3	18.04	0.05
A_52_P851529	RIKEN full-length clone:B230311D12	Mm.153019	AK045794	3	56	3	17.61	0.05
A_52_P139316	Unknown	—	—	9	154	12	17.47	0.07
A_52_P545505	RIKEN full-length clone:A430068J17	Mm.254835	AK079794	4	58	4	16.26	0.06
A_52_P141608	Hypothetical protein E030010A14	Mm.86388	NM_183160	31	488	64	15.89	0.13
A_52_P241917	RIKEN full-length clone:A230074D21	Mm.244393	AK038910	33	499	74	15.35	0.15
A_51_P124362	Defensin beta 9 (*Defb9*)	Mm.171224	NM_139219	4	53	5	15.02	0.10
A_51_P337269	Aldolase 2, B isoform (*Aldob*)	Mm.218862	NM_144903	5	65	5	14.23	0.08

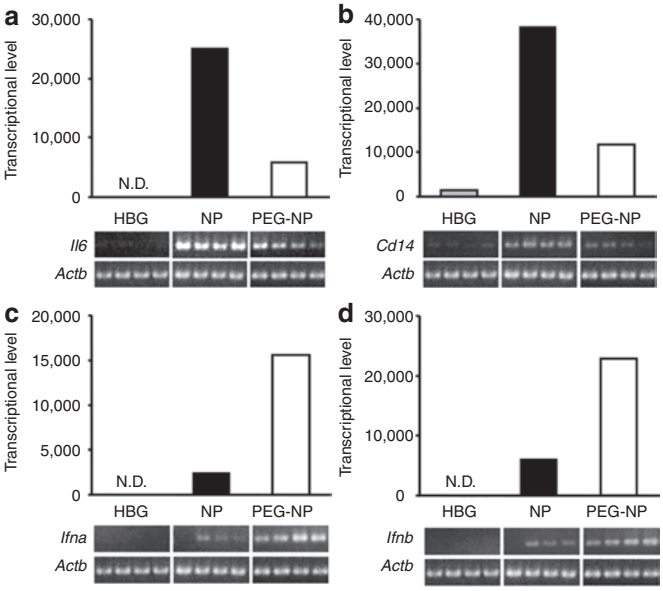

Figure 2 Transcriptional levels obtained by microarray were in agreement with mRNA quantities by quantitative reverse transcriptase-PCR (qRT-PCR). Bars represent transcriptional levels of (**a**) interleukin-6 (*Il6*), (**b**) *Cd14*, (**c**) interferon *Ifna*, and (**d**) *Ifnb* obtained by microarray analysis. Gene expressions were confirmed by semiquantitative RT-PCR as shown in electrophoretic images. qRT-PCR results were in good agreement with the microarray analysis. HBG, HEPES-buffered glucose; NPs, nanoparticles; PEG-NP, PEGylation of NP.

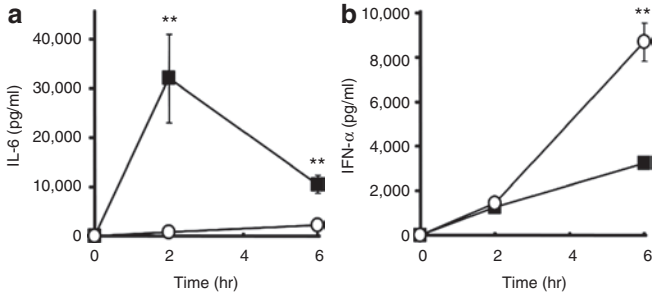

Figure 3 Serum levels of interleukin-6 (IL-6) and interferon (IFN)-α after treatment of nanoparticle (NP) and polyethylene glycol (PEG). Each sample (25 µg plasmid DNA (pDNA)/mouse) was intravenously injected at a normal pressure. At 2 and 6 hours after the intervenous injection (**a**) serum IL-6 and (**b**) IFN-α were evaluated by enzyme-linked immunosorbent (ELISA). (**a**) Nanoparticle (NP) (closed squares) enhanced IL-6 production, and PEGylation (open circles) effectively reduced it. (**b**) On the other hand, PEGylation (open circles) stimulated IFN-α compared to NP (closed squares). Neither IL-6 nor IFN-α were detected in the HEPES-buffered glucose (HBG) treatment. These values are in good agreement with the microarray and reverse transcriptase-PCR results. Data are presented as the mean ± SD (n = 4). $^{**}P < 0.01$. PEG-NP, PEGylation of NP.

related to the immune system and the downregulated genes were associated with mitosis and differentiation, as shown in **Table 2**. These findings suggest that the characteristics between up- and downregulated genes are completely different, presumably because the innate upregulation of a gene related to immune system might turn out to downregulate genes related to the maintenance of cell function such as cytokinesis, mitosis, and cell differentiation. As we assumed, the variation in gene expression including *Il6* and *Ifng* in clusters 1, 3, and 5 (55.8%) showed a tendency for improvement (**Figures 1** and **2**). Serum inflammatory cytokines such as IL-6, TNF-α, and IFN-γ were significantly decreased as the result of PEGylation (**Figure 3** and **Supplementary Figure S1 and Supplementary Materials and Methods**). Therefore, PEGylation appears to contribute to the prevention of inflammatory cytokine production. However, the variation of expression in cluster 2 (42.7%) was equivalent to the level of NP (**Figure 1**). Unexpectedly, the expression of type I IFN in the spleen was conversely aggravated by PEGylation (cluster 4; 1.5%)(**Figures 1** and **2**). As shown in **Figure 3**, the serum level of IFN-α in PEG-NP was equal to or greater than that for NP, in good agreement with the mRNA levels in the spleen. These results suggest that even though PEG is a well known biocompatible macromolecule, PEGylation is not an adequate solution to averting a host response to NPs.

The microarray analysis indicated that PEGylation altered the production of inflammatory cytokine such as *Il6* (better) and type I IFN such as *Ifna* (unchanged or worse) in a different pattern. The question arises as to the cause of the production of inflammatory

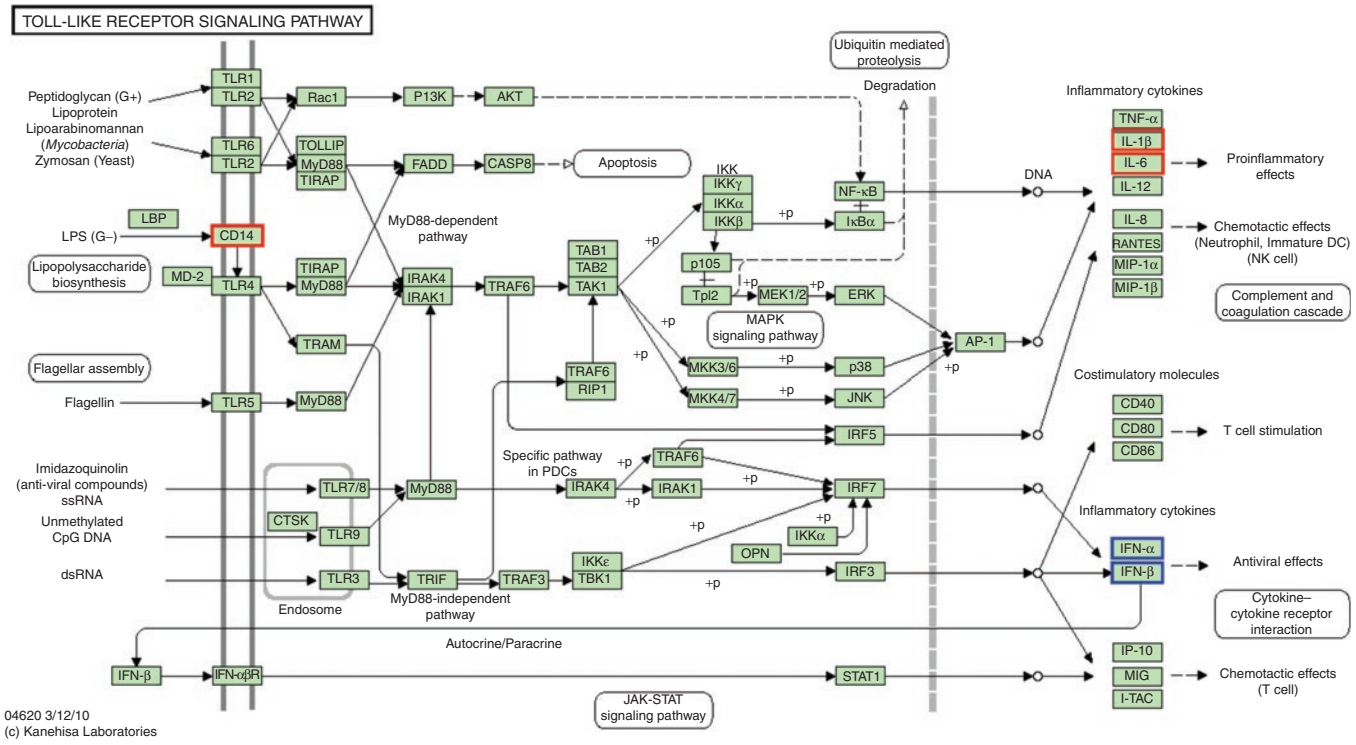

Figure 4 Differentially expressed genes in the toll-like receptor signaling pathway from Kyoto Encyclopedia of Genes and Genomes (KEGG) pathways. Red and blue columns represent differentially expressed genes located in cluster 3 and cluster 4, respectively.

cytokines and type I IFN by NP and PEG-NP. PEG modification under these conditions did not alter the splenic accumulation of NP after systemic administration (**Supplementary Figure S2**). Therefore, the change in cytokine production might be caused after NPs that had arrived in the spleen. The innate immune response to a lipoplex is partially, but not entirely, dependent on the CpG motif in pDNA *via* TLR9, which induces the production of type I IFN and inflammatory cytokines.[6] The plasmid DNA used in this study contains 425 CpG motifs.

Hartman *et al.* previously reported that a pathway analysis following a microarray of Ad revealed that the Myeloid differentiation primary response gene (88) (MyD88) in the TLR signaling pathway plays a major role in the immune response to Ad.[14,15] To elucidate the underlying mechanisms of the response to NP and PEGylated NP, we then focused on the TLR signaling pathway using the Kyoto Encyclopedia of Genes and Genomes database. As a result of the pathway analysis, IL-6, IL-1β, and CD14 in cluster 3, and IFN-α and -β in cluster 4 correspond to the TLR signaling pathway (**Figure 4**). CD14 is a glycosylphosphatidylinositol-anchored cell surface protein that is expressed by phagocytic cells.[32] The recognition of lipopolysaccharide by cells is mediated by the lipopolysaccharide receptor complex, which consists of TLR4, MD2, and CD14.[6] It was observed that CD14 expression by bone marrow granulocytes and odontoblasts was increased by treatment with an agonist for TLR4, such as lipopolysaccharide.[33,34] It was reported that diC14-amidine, a cationic lipid, is assumed to be an agonist for TLR4 due to the association of the acyl chains of diC14-amidine with the hydrophobic pocket in MD2.[35] Empty liposomes using the same lipid component in the envelope of NP showed neither inflammatory cytokine nor type I IFN production after systemic administration (data not shown). Therefore, it is very unlikely that the lipid components used in this study have the potential to function as a TLR4 agonist. However, since *Cd14* expression was significantly altered, an NP that included pDNA would not be irrelevant to a TLR4 mediated immune response. Kedmi *et al.* recently reported that the immune activation of DOTAP based cationic lipid NPs containing siRNA might occur *via* TLR4, which provides support for our prediction.[36]

PEGylation decreased the expression of *Cd14* as shown in **Figure 2b**, presumably because the cationic charge on the surface of the lipid envelope was masked by the PEG layer, which reduced the interaction of NP with biological milieu such as cellular membrane components. On the other hand, as describe above, PEGylation interrupts the intracellular trafficking of nanocarriers, especially in the case of endosomal escape.[24,25] It is quite likely that the exposure time of pDNA to TLR9 in endosomes/lysosomes is prolonged due to the trapping of PEG-NP, which would lead to excess stimulation of TLR9, followed by an enhanced expression of IFN-α and -β. The time difference in the production of IL-6 and IFN-α provides support for our prediction. Inflammatory cytokines such as IL-6 and TNF-α showed a peak response at 2 hour after i.v. administration, and the production dropped rapidly by 6 hour because the interaction of NPs with the cell surface had already occurred, which was followed by the immediate uptake of NPs *via* endocytosis. Although the initial production of IFN-α was slower than that of IL-6, the serum level of IFN-α increased over the 6 hour period after the i.v. injection of PEG-NP due to the prolonged interaction of CpG-DNA with TLR9 in endosomes.

Based on our hypothesis, we examined the effect of accelerating the endosomal escape of PEG-NP with GALA on the type I IFN

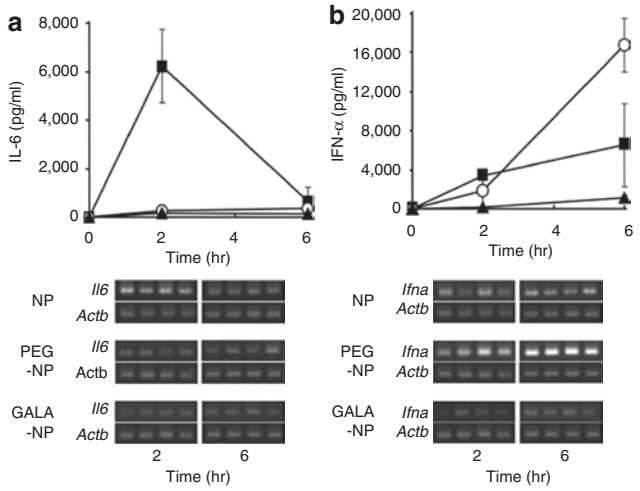

Figure 5 Modification of GALA suppressed interferon (IFN)-α production of PEGylation of NP (PEG-NP). Each sample (25 μg plasmid DNA (pDNA)/mouse) was intravenously injected at a normal pressure. At the indicated time after intervenous injection, serum (**a**) interleukin (IL-6) and (**b**) IFN-α were evaluated by enzyme-linked immunosorbent assay. The gene expression of *Il6* and *Ifna* in the spleen was observed by semiquantitative reverse transcriptase-PCR. Closed squares, open circles, and closed triangles represent NP, PEG-NP, and GALA-NP, respectively. Even though serum IL-6 levels remained at the level in PEG-NP, GALA-NP caused negligible IFN-α production unlike PEG-NP. The gene expression of *Ifna* in the spleen was also decreased by GALA modification. HBG, HEPES-buffered glucose; NPs, nanoparticles; PEG-NP, PEGylation of NP.

production. We previously reported on the successful delivery of either an encapsulated aqueous phase marker, pDNA, or siRNA into the cytosol by introducing GALA on the lipid envelope.[26–28,37] The acceleration in the endosomal escape of NP by GALA almost diminished IFN-α production, and IL-6 remained at low levels (**Figure 5**). The amount of GALA-NP in the spleen was comparable to that for NP and PEG-NP (**Supplementary Figure S2 and Supplementary Materials and Methods**). As an alternate to the use of GALA, PEG detached systems which have the ability to promote the endosomal escape of NPs, are considered to be another potential strategy for reducing type I IFN production in response to intracellular environments with a low pH in endosomes/lysosomes, reducing environment generated by small thiolytical molecules, *e.g.*, glutathione, and enzymes such as cathepsin B.[38–41]

As anther type of DNA sensor, it was reported that DAI (ZBP1) has a role as a cytosolic dsDNA receptor in a CpG-independent manner.[9] In this study, the expression of *Zbp1* located in cluster 2 was increased tenfold by both NP and PEG-NP compared to the control. Although the amount of cytosolic pDNA escaping from endosomes would be increased by presence of GALA, no further immune response occurred. Therefore, the contribution of DAI in the immune response to NP would be minor, and GALA modification could reduce type I IFN production presumably because of the acceleration of endosomal escape. These results lead us to predict that the immune stimulation of NP mediated by TLR9 mainly results in the production of type I IFN in a CpG-dependent manner, whereas that mediated by TLR4 induces inflammatory cytokines in a CpG-independent manner. Although TLR 1/2 and 6 on the cell surface are also linked to inflammatory cytokine production, the involvement with TLR1/2 and 6 are presently unclear. Of course, further studies will be required to completely understand the mechanisms and pathways for the immune response.

In summary, a microarray-based analysis was performed, to explore the mechanism of host responses to systemically administrated NPs. As expected, PEGylation partially reduced the host response to NP. However, PEGylation also stimulated the response of type I IFN to NP. The pathway and mechanism analysis yielded insights into the causes of cytokine production and a strategy for the design of a carrier that can escape specific immune activation. This study provides the first rational strategy for reducing immunological stimulation based on the genome wide microarray analysis of systemically administrated nonviral lipid NPs.

MATERIALS AND METHODS

Materials. Linear PEI (750 kDa) was purchased from SIGMA-Aldrich (St Louis, MO). DOTAP, DOPE, cholesterol, and distearoyl-*sn*-glycero-3-phoshoethanolamine-N-[methoxy (polyethylene glycol)-2000] (PEG-DSPE) were obtained by Avanti Polar Lipid (Alabaster, AL). EndoFree Plasmid Giga Kit and RNeasy Mini Kit were purchased from QIAGEN (Hilden, Germany). RNase-free DNase I was purchased from TAKARA (Otsu, Japan). High Capacity RNA-to-cDNA Kit was obtained from Agilent Technologies (Palo Alto, CA). Male imprinting control region mice (5–6 weeks old) were purchased from CLEA (Tokyo, Japan). Enzyme-linked immunosorbent (ELISA) assay kits of Quantikine Immunoassay mouse IL-6 was purchased from R&D systems (Minneapolis, MN). ELISA assay kits of Verikine Mouse Interferon Alpha ELISA kit was purchased from PBL Biomedical Laboratories (New Brunswick, NJ).

Preparation of pDNA/PEI complex and NPs. pcDNA-3.1(+)-luc was prepared using an Endfree Plasmid Giga Kit, followed by purification with an Endotrap Blue to entirely eliminate traces of endotoxins. To formulate the pDNA/PEI complex, 200 μl of pDNA (0.1 mg/ml) was condensed with 100 μl of PEI (0.6 mmol/l) in 10 mmol/l HEPES buffer (pH 7.4), at a nitrogen/phosphate (N/P) ratio of 1:15. NPs were prepared by the lipid hydration method as reported previously.[42] Briefly, a lipid film was prepared in a glass test tube by evaporating a chloroform solution of lipids, containing DOTAP, DOPE, and cholesterol (300 nmol total lipids in 3:4:3 molar ratio). For modifying of NP with PEG-DSPE or chol-GALA, the lipid film was prepared by evaporation with the indicated amounts of PEG-DSPE or chol-GALA. The lipid film then was hydrated with the 300 μl of pDNA/PEI complex solution for 10 minutes at room temperature, followed by sonication for ~1 minute in a bath-type sonicator (AU-25, AIWA, Tokyo, Japan). The average diameter and the ζ-potential of the condensed pDNA/PEI complex and NPs were determined using a Zetasizer Nano ZS ZEN3600 (MALVERN Instrument, Worchestershire, UK).

Animal experiments. Either the pDNA/PEI complex or NPs were administered to male imprinting control region mice *via* the tail vein, at a dose of 25 μg of pDNA. HBG treatment was used as a control. At the indicated times after injection, blood and spleen tissues were collected. Blood samples were stored for overnight at 4 °C, followed by centrifugation (10,000 rpm, 4 °C, 10 minutes) to obtain serum. Spleen samples were stored in RNA later solution at −20 °C to avoid RNA degradation. The experimental protocols were reviewed and approved by the Hokkaido University Animal Care Committee in accordance with the "Guide for the Care and Use of Laboratory Animals."

Determination of serum cytokine. IL-6 and IFN-α levels in serum were determined with ELISA kits according to the manufacturer's instructions.

Semi-quantitative RT-PCR. A spleen sample was homogenized and total cellular RNA was purified using an RNeasy mini kit. To exclude DNA contamination, the RNA sample was treated with RNA free DNase I.

Approximately 2.0 μg of RNA from each sample was reverse transcribed using a High Capacity RNA-to-cDNA kit by following manufacturer's instructions. PCRs were performed using the following primers: IL-6 (forward: 5′-TCCTCTGGTCTTCTGGAGTA-3′ and primer: 5′-TCCT TAGCCACTCCTTCTGT-3′); CD14 (forward: 5′-CTGATCTCAGCCCTC TGTCC-3′ and reverse: 5′-GCTTCAGCCCAGTGAAAGAC-3′); IFN-α (forward: 5′-GCTGCATGGAATACAACCCT-3′ and reverse: 5′-CTTC TGCTCTGACCACCTCC-3′); IFN-β (forward: 5′-GAGGAAAGATTGAC GTGGGA-3′ and reverse: 5′-ACCACCACTCATTCTGAGGC-3′); β-actin (forward: 5′-ACATGGAGAAGATGTGGCAC-3′ and reverse: 5′-TCCAT CACAATGCCTGTGGT-3′). β-actin was measured as an endogenous reference gene. The PCR thermocycling program was as follows: Denaturation at 94 °C for 30 seconds, annealing at 60 °C for 30 seconds and extension at 70 °C for 30 seconds through 27–32 cycles. The PCR products were electrophoresed through a 2.0% agarose gel and then stained using ethidium bromide and visualized under UV light.

DNA mircoarray experiments. Spleen samples were homogenized and total cellular RNA was purified using an RNeasy mini kit, as described above. Total RNA extracted from four mice spleen (125 ng each) were pooled into one sample (total 500 ng) for normalizing individual differences. The integrity of the pooled total RNA samples was evaluated using an Agilent 2100 Bioanalyzer (Agilent, Foster City, CA). The pooled RNA was labeled with Cy-3 using the Low RNA Input Linear Amplification Kit PLUS, One-Color (Product No. 5188–5339), followed by purification using RNeasy mini kit to eliminate unlabeled Cy-3. Cy-3 labeled RNA sample was then hybridized to Agilent Whole Mouse Genome Microarray (Product No. G4122F) according to manufacturer's hybridization instruction. The microarray slides were analyzed using an Agilent Microarray scanner (Product No. G2565AA). Microarray expression data were obtained using the Agilent Feature Extraction software (Ver A.6.1.1).

Data analysis. Microarray data were analyzed using GeneSpring software version 7.3 (Agilent). Genes were regarded as upregulated when they had a ratio of ≥3 and as downregulated when they had a ratio of ≤0.34 in the administration of NP compared with HBG treatment. To understand the differential gene expression pattern, a hierarchical clustering analysis was performed using a Pearson Correlation and an average linkage clustering algorithm. The GO analysis was performed to assign biological meaning to the subset of gene clusters. Over-representation of genes with altered expression in the NP treatment compared with the HBG treatment within specific GO categories was determined using Fisher's exact probability test. Pathway analysis of TLR signaling pathway was performed by using the Kyoto Encyclopedia of Genes and Genomes pathway map.

Statistical analysis. Comparisons between multiple treatments were made using one-way ANOVA, followed by the Bonferroni test. Pair-wise comparisons between treatments were made using a Student's *t*-test. A *P*-value of <0.05 was considered significant.

SUPPLEMENTARY MATERIAL

Figure S1. Serum levels of (a) IL-6 and (b) IFN-γ (c) TNF-α and (d) ALT.

Figure S2. Accumulation of NPs in the spleen.

Materials and Methods.

ACKNOWLEDGMENTS

This study was supported by Special Coordination Funds for Promoting Science and Technology of the Ministry of Education, Culture, Sports, Science and Technology (MEXT), and Grant for Industrial Technology Research from New Energy and Industrial Technology Development Organization (NEDO), and by Grants-in-Aid for Scientific Research on Priority Areas from the Japan Society for the Promotion of Science (JSPS). We thank M. S. Feather for his helpful advice in writing the English manuscript.

REFERENCES

1. Deakin, CT, Alexander, IE and Kerridge, I (2009). Accepting risk in clinical research: is the gene therapy field becoming too risk-averse? *Mol Ther* **17**: 1842–1848.
2. Li, SD and Huang, L (2006). Gene therapy progress and prospects: non-viral gene therapy by systemic delivery. *Gene Ther* **13**: 1313–1319.
3. Tros de Ilarduya, C, Sun, Y and Düzgünes, N (2010). Gene delivery by lipoplexes and polyplexes. *Eur J Pharm Sci* **40**: 159–170.
4. Osada, K, Christie, RJ and Kataoka, K (2009). Polymeric micelles from poly(ethylene glycol)-poly(amino acid) block copolymer for drug and gene delivery. *J R Soc Interface* **6 Suppl 3**: S325–S339.
5. Whitmore, M, Li, S and Huang, L (1999). LPD lipopolyplex initiates a potent cytokine response and inhibits tumor growth. *Gene Ther* **6**: 1867–1875.
6. Kawai, T and Akira, S (2010). The role of pattern-recognition receptors in innate immunity: update on Toll-like receptors. *Nat Immunol* **11**: 373–384.
7. Zhao, H, Hemmi, H, Akira, S, Cheng, SH, Scheule, RK and Yew, NS (2004). Contribution of toll-like receptor -9 signaling to the acute inflammatory response to nonviral vectors. *Mol Ther* **9**: 241–248.
8. Sakurai, H, Sakurai, F, Kawabata, K, Sasaki, T, Koizumi, N, Huang, H *et al.* (2007). Comparison of gene expression efficiency and innate immune response induced by Ad vector and lipoplex. *J Control Release* **117**: 430–437.
9. Yasuda, K, Ogawa, Y, Yamane, I, Nishikawa, M and Takakura, Y (2005). Macrophage activation by a DNA/cationic liposome complex requires endosomal acidification and TLR9-dependent and -independent pathways. *J Leukoc Biol* **77**: 71–79.
10. Takaoka, A, Wang, Z, Choi, MK, Yanai, H, Negishi, H, Ban, T *et al.* (2007). DAI (DLM-1/ZBP1) is a cytosolic DNA sensor and an activator of innate immune response. *Nature* **448**: 501–505.
11. Yasuda, S, Yoshida, H, Nishikawa, M and Takakura, Y (2010). Comparison of the type of liposome involving cytokine production induced by non-CpG Lipoplex in macrophages. *Mol Pharm* **7**: 533–542.
12. Shayakhmetov, DM, Di Paolo, NC and Mossman, KL (2010). Recognition of virus infection and innate host responses to viral gene therapy vectors. *Mol Ther* **18**: 1422–1429.
13. McCaffrey, AP, Fawcett, P, Nakai, H, McCaffrey, RL, Ehrhardt, A, Pham, TT *et al.* (2008). The host response to adenovirus, helper-dependent adenovirus, and adeno-associated virus in mouse liver. *Mol Ther* **16**: 931–941.
14. Hartman, ZC, Kiang, A, Everett, RS, Serra, D, Yang, XY, Clay, TM *et al.* (2007). Adenovirus infection triggers a rapid, MyD88-regulated transcriptome response critical to acute-phase and adaptive immune responses in vivo. *J Virol* **81**: 1796–1812.
15. Hartman, ZC, Black, EP and Amalfitano, A (2007). Adenoviral infection induces a multi-faceted innate cellular immune response that is mediated by the toll-like receptor pathway in A549 cells. *Virology* **358**: 357–372.
16. Omidi, Y, Hollins, AJ, Drayton, RM and Akhtar, S (2005). Polypropylenimine dendrimer-induced gene expression changes: the effect of complexation with DNA, dendrimer generation and cell type. *J Drug Target* **13**: 431–443.
17. Omidi, Y, Hollins, AJ, Benboubetra, M, Drayton, R, Benter, IF and Akhtar, S (2003). Toxicogenomics of non-viral vectors for gene therapy: a microarray study of lipofectin- and oligofectamine-induced gene expression changes in human epithelial cells. *J Drug Target* **11**: 311–323.
18. Tagami, T, Hirose, K, Barichello, JM, Ishida, T and Kiwada, H (2008). Global gene expression profiling in cultured cells is strongly influenced by treatment with siRNA-cationic liposome complexes. *Pharm Res* **25**: 2497–2504.
19. Beyerle, A, Irmler, M, Beckers, J, Kissel, T and Stoeger, T (2010). Toxicity pathway focused gene expression profiling of PEI-based polymers for pulmonary applications. *Mol Pharm* **7**: 727–737.
20. Kogure, K, Akita, H, Yamada, Y and Harashima, H (2008). Multifunctional envelope-type nano device (MEND) as a non-viral gene delivery system. *Adv Drug Deliv Rev* **60**: 559–571.
21. Cesta, MF (2006). Normal structure, function, and histology of the spleen. *Toxicol Pathol* **34**: 455–465.
22. Alexis, F, Pridgen, E, Molnar, LK and Farokhzad, OC (2008). Factors affecting the clearance and biodistribution of polymeric nanoparticles. *Mol Pharm* **5**: 505–515.
23. Hafez, IM and Cullis, PR (2001). Roles of lipid polymorphism in intracellular delivery. *Adv Drug Deliv Rev* **47**: 139–148.
24. Mishra, S, Webster, P and Davis, ME (2004). PEGylation significantly affects cellular uptake and intracellular trafficking of non-viral gene delivery particles. *Eur J Cell Biol* **83**: 97–111.
25. Remaut, K, Lucas, B, Braeckmans, K, Demeester, J and De Smedt, SC (2007). Pegylation of liposomes favours the endosomal degradation of the delivered phosphodiester oligonucleotides. *J Control Release* **117**: 256–266.
26. Sasaki, K, Kogure, K, Chaki, S, Nakamura, Y, Moriguchi, R, Hamada, H *et al.* (2008). An artificial virus-like nano carrier system: enhanced endosomal escape of nanoparticles *via* synergistic action of pH-sensitive fusogenic peptide derivatives. *Anal Bioanal Chem* **391**: 2717–2727.
27. Sakurai, Y, Hatakeyama, H, Akita, H, Oishi, M, Nagasaki, Y, Futaki, S *et al.* (2009). Efficient short interference RNA delivery to tumor cells using a combination of octaarginine, GALA and tumor-specific, cleavable polyethylene glycol system. *Biol Pharm Bull* **32**: 928–932.
28. Hatakeyama, H, Ito, E, Akita, H, Oishi, M, Nagasaki, Y, Futaki, S *et al.* (2009). A pH-sensitive fusogenic peptide facilitates endosomal escape and greatly enhances the gene silencing of siRNA-containing nanoparticles *in vitro* and in vivo. *J Control Release* **139**: 127–132.
29. Li, W, Nicol, F and Szoka, FC Jr (2004). GALA: a designed synthetic pH-responsive amphipathic peptide with applications in drug and gene delivery. *Adv Drug Deliv Rev* **56**: 967–985.
30. Kawakami, S, Ito, Y, Charoensit, P, Yamashita, F and Hashida, M (2006). Evaluation of proinflammatory cytokine production induced by linear and branched polyethylenimine/plasmid DNA complexes in mice. *J Pharmacol Exp Ther* **317**: 1382–1390.

31. Saito, Y, Higuchi, Y, Kawakami, S, Yamashita, F and Hashida, M (2009). Immunostimulatory characteristics induced by linear polyethyleneimine-plasmid DNA complexes in cultured macrophages. *Hum Gene Ther* **20**: 137–145.
32. Freudenberg, MA, Tchaptchet, S, Keck, S, Fejer, G, Huber, M, Schütze, N *et al.* (2008). Lipopolysaccharide sensing an important factor in the innate immune response to Gram-negative bacterial infections: benefits and hazards of LPS hypersensitivity. *Immunobiology* **213**: 193–203.
33. Botero, TM, Shelburne, CE, Holland, GR, Hanks, CT and Nör, JE (2006). TLR4 mediates LPS-induced VEGF expression in odontoblasts. *J Endod* **32**: 951–955.
34. Pedron, T, Girard, R, Inoue, K, Charon, D and Chaby, R (1997). Lipopolysaccharide and the glycoside ring of staurosporine induce CD14 expression on bone marrow granulocytes by different mechanisms. *Mol Pharmacol* **52**: 692–700.
35. Tanaka, T, Legat, A, Adam, E, Steuve, J, Gatot, JS, Vandenbranden, M *et al.* (2008). DiC14-amidine cationic liposomes stimulate myeloid dendritic cells through Toll-like receptor 4. *Eur J Immunol* **38**: 1351–1357.
36. Kedmi, R, Ben-Arie, N and Peer, D (2010). The systemic toxicity of positively charged lipid nanoparticles and the role of Toll-like receptor 4 in immune activation. *Biomaterials* **31**: 6867–6875.
37. Kakudo, T, Chaki, S, Futaki, S, Nakase, I, Akaji, K, Kawakami, T *et al.* (2004). Transferrin-modified liposomes equipped with a pH-sensitive fusogenic peptide: an artificial viral-like delivery system. *Biochemistry* **43**: 5618–5628.
38. Li, W, Huang, Z, MacKay, JA, Grube, S and Szoka, FC Jr (2005). Low-pH-sensitive poly(ethylene glycol) (PEG)-stabilized plasmid nanolipoparticles: effects of PEG chain length, lipid composition and assembly conditions on gene delivery. *J Gene Med* **7**: 67–79.
39. Shin, J, Shum, P and Thompson, DH (2003). Acid-triggered release *via* dePEGylation of DOPE liposomes containing acid-labile vinyl ether PEG-lipids. *J Control Release* **91**: 187–200.
40. Zalipsky, S, Qazen, M, Walker, JA 2nd, Mullah, N, Quinn, YP and Huang, SK (1999). New detachable poly(ethylene glycol) conjugates: cysteine-cleavable lipopolymers regenerating natural phospholipid, diacyl phosphatidylethanolamine. *Bioconjug Chem* **10**: 703–707.
41. Zhang, JX, Zalipsky, S, Mullah, N, Pechar, M and Allen, TM (2004). Pharmaco attributes of dioleoylphosphatidylethanolamine/cholesterylhemisuccinate liposomes containing different types of cleavable lipopolymers. *Pharmacol Res* **49**: 185–198.
42. Hatakeyama, H, Akita, H, Kogure, K, Oishi, M, Nagasaki, Y, Kihira, Y *et al.* (2007). Development of a novel systemic gene delivery system for cancer therapy with a tumor-specific cleavable PEG-lipid. *Gene Ther* **14**: 68–77.